MOLECULAR AND CELLULAR BIOLOGY, Aug. 2006, p. 5908–5920 Vol. 26, No. 15
0270-7306/06/$08.00+0 doi:10.1128/MCB.00269-06

Synaptic Plasticity Deficits and Mild Memory Impairments in Mouse Models of Chronic Granulomatous Disease

Kenneth T. Kishida,[1] Charles A. Hoeffer,[2] Daoying Hu,[2] Maryland Pao,[3] Steven M. Holland,[4] and Eric Klann[1,2]*

Department of Neuroscience, Baylor College of Medicine, Houston, Texas 77030[1]; Department of Molecular Physiology and Biophysics, Baylor College of Medicine, Houston, Texas 77030[2]; Office of the Clinical Director, National Institute of Mental Health, National Institutes of Health, Bethesda, Maryland 20892[3]; and Laboratory of Clinical Infectious Diseases, National Institute of Allergy and Infectious Diseases, National Institutes of Health, Bethesda, Maryland 20892[4]

Received 13 February 2006/Returned for modification 13 March 2006/Accepted 15 May 2006

Reactive oxygen species (ROS) are required in a number of critical cellular signaling events, including those underlying hippocampal synaptic plasticity and hippocampus-dependent memory; however, the source of ROS is unknown. We previously have shown that NADPH oxidase is required for *N*-methyl-D-aspartate (NMDA) receptor-dependent signal transduction in the hippocampus, suggesting that NADPH oxidase may be required for NMDA receptor-dependent long-term potentiation (LTP) and hippocampus-dependent memory. Herein we present the first evidence that NADPH oxidase is involved in hippocampal synaptic plasticity and memory. We have found that pharmacological inhibitors of NADPH oxidase block LTP. Moreover, mice that lack the NADPH oxidase proteins gp91^{phox} and p47^{phox}, both of which are mouse models of human chronic granulomatous disease (CGD), also lack LTP. We also found that the gp91^{phox} and p47^{phox} mutant mice have mild impairments in hippocampus-dependent memory. The gp91^{phox} mutant mice exhibited a spatial memory deficit in the Morris water maze, and the p47^{phox} mutant mice exhibited impaired context-dependent fear memory. Taken together, our results are consistent with NADPH oxidase being required for hippocampal synaptic plasticity and memory and are consistent with reports of cognitive dysfunction in patients with CGD.

Chronic granulomatous disease (CGD) is caused by inherited mutations in genes encoding subunits of the NADPH oxidase complex (7, 14, 36, 43). NADPH oxidase is composed of two membrane-bound subunits (gp91^{phox} and p22^{phox}) and three cytosolic subunits, which include p47^{phox}, p67^{phox}, and Rac (49). The membrane-bound subunits form a heterodimer that stabilizes them within the membrane, whereas the cytosolic subunits are recruited to the membrane following stimulation. Complete complex assembly is necessary for full NADPH oxidase activity (2). Mutations in the gp91^{phox} and p47^{phox} genes are the most common mutations that cause CGD (58). These mutations disable the NADPH oxidase complex, thereby preventing the oxidation of NADPH and the subsequent production of superoxide (31, 45), which is required for pathogen destruction as well as most superoxide-dependent signal transduction in nonphagocytic cells (21, 24, 49).

CGD patients suffer from frequent bacterial and fungal infections and inflammatory granulomas in the lungs, liver, skin, lymph nodes, and lining of the gastrointestinal and genitourinary tracts (34); loss of phagocytic oxidative burst activity due to mutations in genes encoding the NADPH oxidase subunits is the cause of these symptoms. gp91^{phox} (40) and p47^{phox} (22) mutant mice have been generated and used as models for the most common mutations that cause CGD. These mutant mouse lines, which lack their respective gene products due to targeted homologous recombinant gene disruption, have been utilized to understand the molecular mechanisms underlying CGD (22, 40).

NADPH oxidase has been studied primarily for its role in the phagocyte oxidative burst in the immune system (43); however, its regulation and expression pattern suggest that it may be an important source of superoxide in the brain (9, 46, 54). Interestingly, some CGD patients also suffer from cognitive dysfunction (37), indicating that the lack of a fully functional NADPH oxidase impairs higher-order brain function. NADPH oxidase function in the nervous system has been well studied in microglia (9), and a role for NADPH oxidase in astrocyte function has been described (1). Moreover, it has been demonstrated that NADPH oxidase is expressed in neurons (51, 54) and localized at synapses (51). These findings indicate that NADPH oxidase may be a source of superoxide that is required for normal brain function.

Superoxide is known to be required for hippocampal synaptic plasticity, specifically long-term potentiation (LTP) (25–27, 52, 53), as well as hippocampus-dependent memory (27, 52, 53). However, the source of superoxide required for LTP and memory formation has yet to be determined. We previously have shown that superoxide is required for *N*-methyl-D-aspartate (NMDA) receptor-dependent activation of extracellular signal-regulated kinase (ERK) in the hippocampus (24) and that a likely source of superoxide required for ERK activation is NADPH oxidase (24). Thus, we hypothesized that NADPH oxidase could be a source of superoxide that is required for hippocampal LTP and memory. In order to test this hypothesis directly, we examined LTP in hippocampal slices treated with two structurally and functionally different NADPH oxidase

* Corresponding author. Mailing address: Department of Molecular Physiology & Biophysics, Baylor College of Medicine, One Baylor Plaza BCM 335, Houston, TX 77030. Phone: (713) 798-5630. Fax: (713) 798-3475. E-mail: eklann@bcm.tmc.edu.

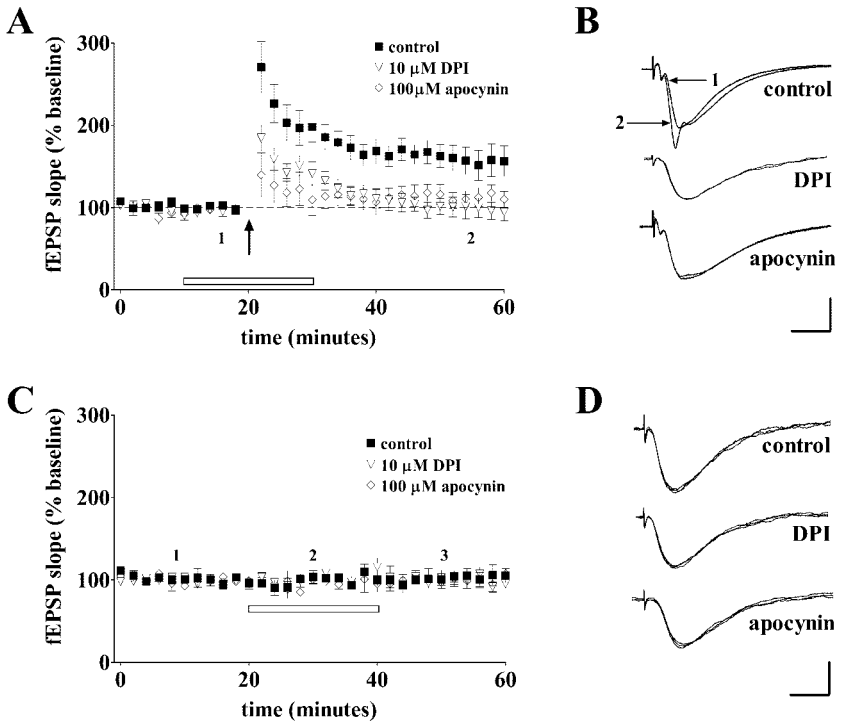

FIG. 1. NADPH oxidase inhibitors block HFS-induced E-LTP. (A) A single 1-second 100-Hz train of HFS (indicated by the arrow) induced E-LTP in vehicle-treated wild-type hippocampal slices (control) but was blocked when HFS was delivered in the presence of either 10 μM DPI or 100 μM apocynin ($n = 8$ slices; four mice per treatment) ($P < 0.0001$ by one-way ANOVA) (apocynin versus control, $P < 0.001$; DPI versus control, $P < 0.001$; DPI versus apocynin, $P > 0.05$ by Newman-Keuls multiple comparison test). (B) Two representative fEPSP recordings from time points 1 and 2 in panel A were overlaid to demonstrate potentiation in control slices, which was absent in drug-treated slices. (C) Control slices with or without either 10 μM DPI or 100 μM apocynin applied to slices for 20 min while recording fEPSPs; 10 μM DPI or 100 μM apocynin did not affect baseline fEPSPs ($P > 0.05$ by one-way ANOVA). (D) Three representative fEPSPs from time points 1, 2, and 3 in panel C were overlaid, demonstrating the lack of change in baseline responses during 1 hour of recording with or without application of either 10 μM DPI or 100 μM apocynin for 20 min.

inhibitors. We also examined LTP in hippocampal slices prepared from either gp91^{phox} or p47^{phox} mutant mice. In addition, we tested the ability of the NADPH oxidase mutant mice to perform hippocampus-dependent learning and memory tasks. Our data indicate that the loss of a functional NADPH oxidase results in deficient LTP and mild hippocampus-dependent memory impairments. Our data are the first to show a direct role of NADPH oxidase involvement in hippocampal synaptic plasticity and memory formation. Overall, these findings are consistent with the idea that superoxide produced by NADPH oxidase is required for normal hippocampal synaptic plasticity and memory and may explain why some CGD patients exhibit cognitive dysfunction.

MATERIALS AND METHODS

Animal breeding and colony maintenance. All mice were housed in Baylor College of Medicine's Transgenic Mouse Facility, which is a level III barrier facility; the housing unit for the mice used in these experiments was deemed pathogen free throughout the duration of the experiments presented here. Cages, bedding, water, and feed were sterilized and changed regularly by technical staff, thus maintaining the pathogen-free environment necessary to carry out these experiments. All cages contained corncob bedding, and HEPA-filtered air was pumped in continuously. The gp91^{phox} and p47^{phox} knockout (KO) mice were generated as previously described (22, 40) and were maintained in a C57BL/6 background (backcrossed more than 10 generations). All wild-type animals used also were from the same C57BL/6 strain. PCR was performed to determine the genotype of experimental mice as described elsewhere (20). All experiments involving the gp91^{phox} KO line were performed in males, whereas male and female mice were used for experiments in the p47^{phox} KO mice. Wild-type littermates were used as controls in all experiments with KO mice. All experiments were performed in accordance with IACUC guidelines.

Electrophysiology. Hippocampi from 2- to 3-month-old wild-type, gp91^{phox} KO, and p47^{phox} KO mice were removed, and 400-μm slices were prepared using a tissue chopper as previously described (24). The slices were perfused for 1 to 2 h with oxygenated artificial cerebrospinal fluid (ACSF; in mM: 125 NaCl, 2.5 KCl, 1.25 NaH_2PO_4, 25 $NaHCO_3$, 25 D-glucose, 2 $CaCl_2$, and 1 $MgCl_2$) in an interface tissue slice chamber at 30°C. A bipolar stimulating electrode was placed to stimulate the Schaffer collaterals emanating from CA3 pyramidal neurons, and the recording electrode was placed in the stratum radiatum in area CA1.

Input/output. In order to determine the response range for each hippocampal slice, the stimulus range was divided into 10 arbitrary units. The slices were stimulated at each level, and the field excitatory postsynaptic potential (fEPSP) was recorded. Within each fEPSP waveform, the fiber volley was used to determine the input value (amplitude of the fiber volley). The range of input values and their respective output values (measured as the fEPSP slope) were plotted as a means to characterize basal synaptic transmission in mutant mice and wild-type littermates across all experiments performed. At the start of each experiment, the maximal fEPSP response was determined, as was the stimulation intensity that elicited 30 to 50% of the maximal fEPSP response. No differences were found between wild-type littermates of the gp91^{phox} KO and wild-type littermates of the p47^{phox} KO mice and, thus, these animals were grouped for further analyses.

Baseline responses. Baseline responses were collected using the stimulation intensity which elicited 30 to 50% of the maximal fEPSP response as determined by the input-output relationship described above. Data points were collected every 2 minutes as the average response of six fEPSPs collected every 20 seconds.

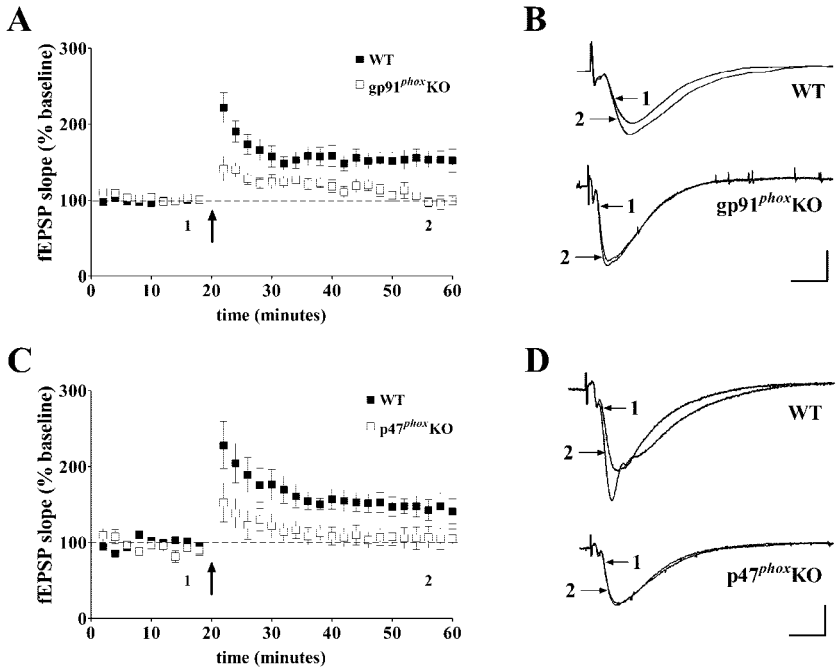

FIG. 2. NADPH oxidase mutant mice do not express HFS-induced E-LTP. (A) A single 1-second 100-Hz train of HFS (indicated by the arrow) induced E-LTP in wild-type mice but failed to induce LTP in gp91^{phox} KO mice (n = 11 slices; five mice per genotype) ($P < 0.0001$ by two-way ANOVA). (B) Two representative fEPSPs from time points 1 and 2 in panel A were overlaid to demonstrate potentiation in slices prepared from wild-type mice, which was absent in slices prepared from gp91^{phox} KO mice. (C) A single 1-second 100-Hz train of HFS (indicated by the arrow) induced E-LTP in wild-type mice but failed to induce E-LTP in p47^{phox} KO mice (n = 8 slices; four mice per genotype) ($P < 0.0001$ by two-way ANOVA). (D) Two representative fEPSPs from time points 1 and 2 in panel C were overlaid to demonstrate potentiation in slices prepared from wild-type mice, which was absent in slices prepared from p47^{phox} KO mice.

Induction of LTP. Following 20 min of baseline recording, a single high-frequency stimulus (HFS) at maximal intensity (100 Hz for 1 s) was delivered. Following the HFS, recordings resumed for 45 min. Long-lasting LTP (L-LTP) was elicited using a previously described L-LTP induction protocol (3); briefly, four trains of HFS (100 Hz for 1 s) spaced 5 min apart were delivered following a 20-min baseline. Potentiated responses were then tracked for 3 h.

Pharmacology. Baseline responses were recorded for 20 min before the addition of either diphenylene iodonium (DPI) or apocynin. Then, either vehicle, 10 μM DPI, or 100 μM apocynin was applied for 20 min while the recordings continued. For LTP experiments, a single HFS (as described above) was delivered 10 min after the application of the pharmacological agent. Following the 20-min application, the pharmacological agent was removed and the recordings continued for the indicated amount of time.

PTP. Posttetanic potentiation (PTP) was induced with a single train of HFS (100 Hz for 1 second) in the presence of 2-amino-5-phosphonovaleric acid (APV; 100 μM) in ACSF. fEPSPs were recorded every 20 seconds for 2 minutes prior to the HFS and every second for 15 seconds immediately post-HFS. After the initial 15 seconds post-HFS, fEPSPs were recorded for 2 min, 5 min post-HFS. Single fEPSP traces collected at each time point were used to measure the slope of the fEPSP, which was plotted as the mean ± the standard error of the mean over multiple trials over the time course of the experiment. PTP values in the wild-type littermates for each of the mutant mice were not significantly different from each other and thus were grouped for further analysis and presentation.

PPF. Paired-pulse facilitation (PPF), a presynaptic facilitation, was induced with two stimuli of equal intensity (same as baseline intensity) presented in rapid succession at variable interpulse intervals ranging from 10 ms to 400 ms. PPF was measured by examining the ratio of the fEPSP slope of stimulus 2 to that of stimulus 1. PPF values in the wild-type littermates from each of the mutant mice were not significantly different from each other and thus were grouped for data presentation.

Isolation of NMDA receptor-mediated fEPSPs. Baseline fEPSPs were collected as described above. Subsequently, ACSF containing 0 mM $MgCl_2$ and 4 mM $CaCl_2$ was applied to elicit mixed AMPA (α-amino-3-hydroxy-5-methyl-4-isoxazolepropionic acid) and NMDA receptor-mediated fEPSPs. CNQX (6-cyano-2,3-dihydroxy-7-nitro-quinoxaline) at 20 μM then was applied to isolate NMDA receptor-mediated fEPSPs. Confirmation that the remaining fEPSP was mediated by NMDA receptors was obtained by applying 100 μM APV, which completely abolished any remaining fEPSP response.

Synaptic fatigue analysis. Baseline fEPSPs were collected as described above. APV at 100 μM was applied to the slices for at least 20 min prior to the delivery of a 10-Hz stimulation protocol that lasted 3 seconds. The resultant fEPSPs were recorded during the stimulation protocol and analyzed.

Conditioned fear. Associative memory was assessed using the conditioned fear paradigm. The training sessions for contextual and cued conditioned fear consisted of a 2-min exploratory period followed by two conditioned stimulus-unconditioned stimulus pairings (a 30-s, 90-db white noise tone and a 2-s, 0.9-mA foot shock at the end of the tone) separated by 1 minute. Contextual tests were performed in the training chamber 24 h later. Cue testing was performed in a distinct chamber 25 h following training. Baseline freezing behavior was monitored for 3 minutes prior to the presentation of the testing tone (3-min, 90-db white noise tone). Freezing behavior was monitored throughout the testing phases to compare fearful responses to the contextual and cued conditional stimuli across wild-type and mutant mice.

MWM. Spatial learning and memory were tested using the Morris water maze (MWM). During the training phase, mice were given four trials each day (60-second maximum duration per trial, with an intertrial interval of at least 20 min) for four consecutive days followed by a single probe trial (testing trial) on the fifth day. The training and probe trial regimen was repeated once for a total of 10 days of experimentation (4 days of training, 1 day of testing, 4 days of training, and 1 day of testing). The latency to find the platform was recorded for each training day. For each of the probe trials, the platform was removed and the number of times the mice crossed over where the platform had been was recorded during a 1-minute trial, as was the time spent in each of the four quadrants in the pool. All data were collected digitally using a charge-coupled device camera placed directly over the pool and coupled with video tracking software (Noldus EthoVision System).

Rotating rod. Motor coordination, balance, and memory were tested using an accelerating rotating rod (Ugo Basile Biological Research Apparatus, Italy) (38). Mice were tested repeatedly on two consecutive days, four trials per day, and the time the mice were able to remain balanced on the rotating rod was recorded.

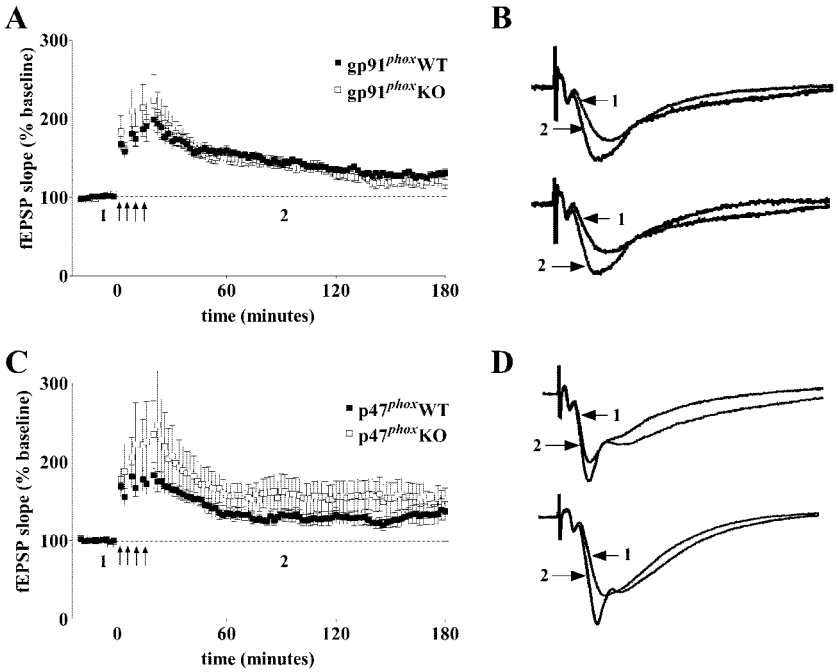

FIG. 3. NADPH oxidase mutant mice express L-LTP. (A) Four trains of HFS (1 second at 100 Hz; indicated by the arrows) spaced 5 min apart induced L-LTP in wild-type mice and in gp91^{phox} KO mice (n = 8 slices; eight mice per genotype) ($P > 0.05$ by two-way ANOVA). (B) Two representative fEPSPs from time points 1 and 2 in panel A were overlaid to demonstrate potentiation in slices prepared from wild-type and gp91^{phox} KO mice. (C) L-LTP in wild-type mice and slightly enhanced L-LTP in p47^{phox} KO mice (n = 7 slices; seven mice per genotype) ($P < 0.0001$ by two-way ANOVA). (D) Two representative fEPSPs from time points 1 and 2 in panel C were overlaid to demonstrate potentiation in slices prepared from wild-type and gp91^{phox} KO mice.

Open field analysis. Locomotor activity was assessed as described previously (38). Data were collected in 2-minute intervals over a 30-minute test session using Versamax software (Accuscan Inc., Columbus, OH) for data collection and analysis. Total distance (in cm) traveled during the assay was measured. Center distance was divided by the total distance to obtain a center distance/total distance ratio. Vertical activity (rearing, measured by the number of photobeam interruptions) and horizontal activity (locomotor activity, measured by the number of photobeam interruptions) also were measured.

Nissl staining. Mice were perfused with 4% paraformaldehyde in phosphate-buffered solution, and brains were prepared for cryostat sectioning as previously described (12). Twenty-micrometer sections were collected using a cryostat and mounted on plus-superfrost glass slides. Sections then were prepared, stained with cresyl violet, and mounted. Images were collected using an inverted light microscope equipped with a digital camera connected to a computer. Images then were cropped and rotated for presentation using Adobe Photoshop.

Data analysis. The results for all experiments are presented as means ± the standard errors of the means. For comparisons between two groups, a two-tailed Student's t test was used. All time course experiments involving multiple comparisons were analyzed using either a one-way or two-way analysis of variance (ANOVA) and, when appropriate, were followed by posttests. Error probabilities with P values of <0.05 were considered statistically significant.

RESULTS

Pharmacological inhibition of NADPH oxidase blocks LTP. It previously was shown that superoxide is required for NMDA receptor-dependent activation of ERK (24) as well as NMDA receptor-dependent HFS-induced LTP in area CA1 of the hippocampus (25, 26, 53). It also was shown that pharmacological inhibition of NADPH oxidase inhibits NMDA receptor-dependent activation of ERK in hippocampal slices (24). Therefore, we hypothesized that NADPH oxidase is a source of the superoxide that is required for NMDA receptor-dependent synaptic plasticity in the hippocampus. We found that LTP was impaired by DPI and apocynin (Fig. 1A and B), two structurally and functionally distinct NADPH oxidase inhibitors (6, 16, 48). Neither DPI nor apocynin altered baseline synaptic transmission (Fig. 1C and D). These data indicate that pharmacological inhibition of NADPH oxidase specifically blocks LTP in the hippocampus, leaving basal synaptic transmission intact.

LTP is blocked in mouse models of CGD. We next investigated LTP in two mouse models of CGD, gp91^{phox} and p47^{phox} KO mice. Both of these NADPH oxidase mutant mouse lines have been shown to lack NADPH oxidase-dependent superoxide production (22, 40). We found that LTP was completely abrogated in hippocampal slices from the gp91^{phox} (Fig. 2A and B) and p47^{phox} (Fig. 2C and D) KO mice compared to their respective wild-type littermates. Taken together with the results from the experiments with the NADPH oxidase inhibitors in Fig. 1, these findings indicate that NADPH oxidase is required for LTP in hippocampal area CA1.

L-LTP is expressed in mouse models of CGD. Previous work investigating the role of superoxide in LTP showed that LTP induced using a single train of HFS, typically called early-phase LTP (E-LTP), is susceptible to scavenging of superoxide, whereas multiple trains of HFS that result in a long-lasting form of LTP, L-LTP, are intact in the presence of superoxide scavengers (25, 26, 53). Thus, we examined L-LTP in slices from gp91^{phox} KO (Fig. 3A and B) and p47^{phox} KO (Fig. 3C and D) mice. Consistent with previous experiments with superoxide scavengers, we observed that L-LTP in gp91^{phox} KO mice

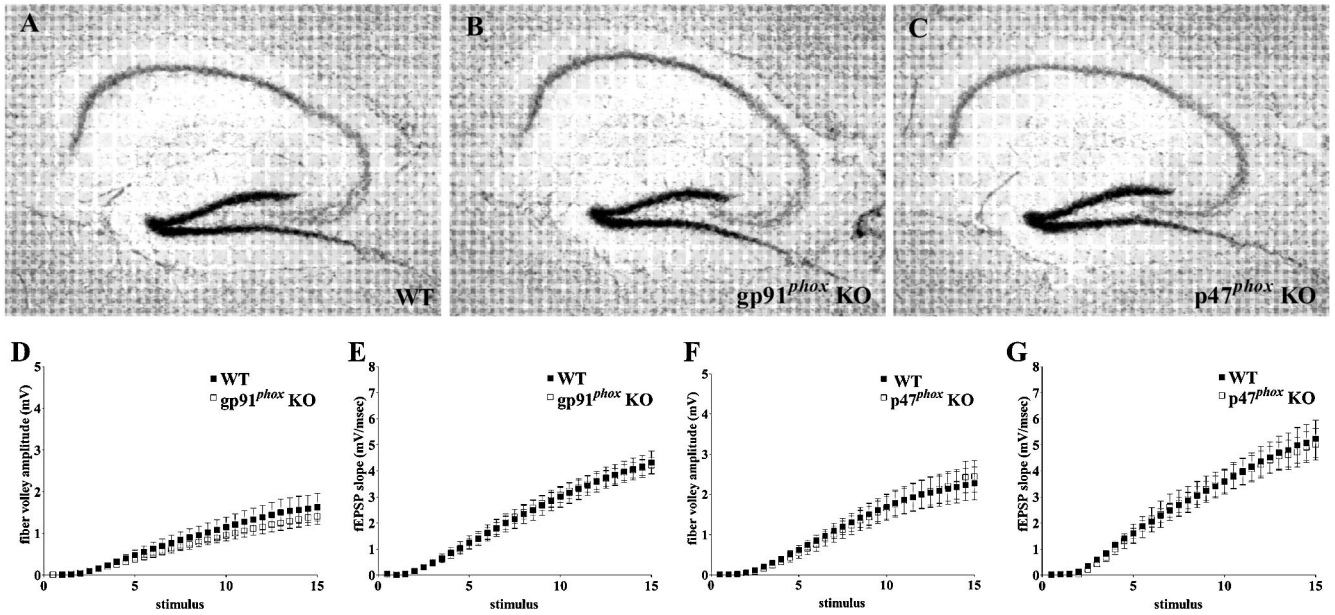

FIG. 4. Normal hippocampal morphology and synaptic transmission in NADPH oxidase mutant mice. (A to C) Nissl-stained sagittal sections from the brains of adult wild-type (A), gp91^{phox} KO (B), and p47^{phox} KO (C) mice. Magnification, ×25. (D to G) The input-output relationship of hippocampal slices is similar between mutant animals and wild-type littermates (for all comparisons, $P > 0.05$ by two-way ANOVA for genotype and stimulus strength). (D) Fiber volley amplitude plotted against stimulus strength for wild-type (filled squares) and gp91^{phox} KO (open squares) mice. (E) fEPSP slope plotted against stimulus strength for wild-type (filled squares) and gp91^{phox} KO (open squares) mice. (F) Fiber volley amplitude plotted against stimulus strength for wild-type (filled squares) and p47^{phox} KO (open squares) mice. (G) fEPSP slope plotted against stimulus strength for wild-type (filled squares) and p47^{phox} KO (open squares) mice.

was normal compared to wild-type littermates (Fig. 3A). Interestingly, p47^{phox} KO mice showed slightly enhanced L-LTP (Fig. 3C). Thus, in contrast to the requirement of both superoxide and NADPH oxidase for E-LTP, our results indicate that neither superoxide nor NADPH oxidase is required for L-LTP.

Hippocampal morphology and basal synaptic transmission are normal in mouse models of CGD. To determine whether the impairment in LTP in the NADPH oxidase mutant mice was caused by either abnormal hippocampal structure or synaptic dysfunction, we examined the gross structure and synaptic transmission in the hippocampi from the gp91^{phox} KO and p47^{phox} KO mice. Nissl staining indicated that there were no obvious differences in the gross morphology of hippocampi from the gp91^{phox} KO and p47^{phox} KO mice compared to their respective wild-type littermates (Fig. 4A to C and data not shown). Moreover, basal synaptic transmission in hippocampal area CA1 was normal in the gp91^{phox} KO and p47^{phox} KO mice as evidenced by similar synaptic input-output relationships in the mutant mice and their wild-type littermates (Fig. 4D to G). These data are consistent with the conclusion that mouse models of CGD have normal gross hippocampal structure and normal synaptic transmission.

NMDA receptor function is normal in mouse models of CGD. It is possible that the E-LTP deficits observed in the p47^{phox} and gp91^{phox} KO mice are caused by alterations of NMDA receptor function. To determine whether NMDA receptor function is altered in the mutant mice, we isolated NMDA receptor-mediated excitatory fEPSPs in area CA1 of hippocampal slices prepared from p47^{phox} KO and gp91^{phox} KO mice, as well as their respective wild-type littermates. Isolated NMDA receptor-mediated fEPSPs were not altered in hippocampal slices prepared from either of the NADPH oxidase mutant mice compared to their wild-type littermates (Fig. 5). Taken together, these data suggest that genetic inhibition of

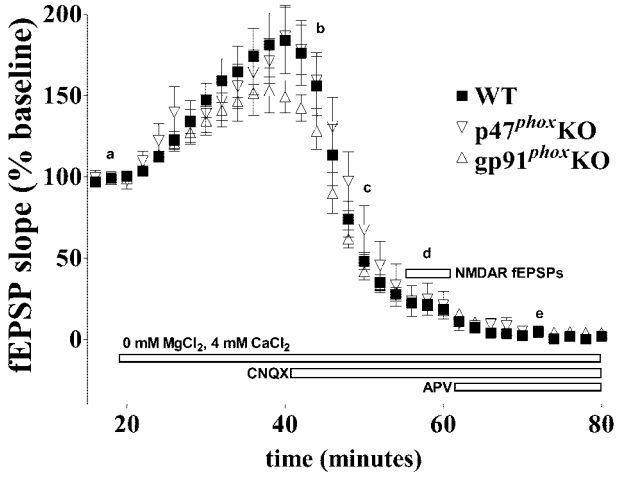

FIG. 5. Normal NMDA receptor-mediated fEPSPs in NADPH oxidase mutant mice: isolation of NMDA receptor-mediated fEPSPs recorded in hippocampal area CA1. The change in fEPSP slope was monitored over time and plotted as a percentage of the baseline fEPSP. No significant difference was observed between NMDA receptor-mediated fEPSPs ($P > 0.05$, one-way ANOVA between all treatments). a, baseline fEPSP; b, fEPSP slope in the presence of 4 mM $CaCl_2$ and 0 mM $MgCl_2$; c, fEPSP after the addition of 20 μM CNQX; d, NMDA receptor-mediated fEPSPs verified by their sensitivity to 100 μM APV; e, fEPSP after the addition of 100 μM APV. $n = 8$ for each experimental condition.

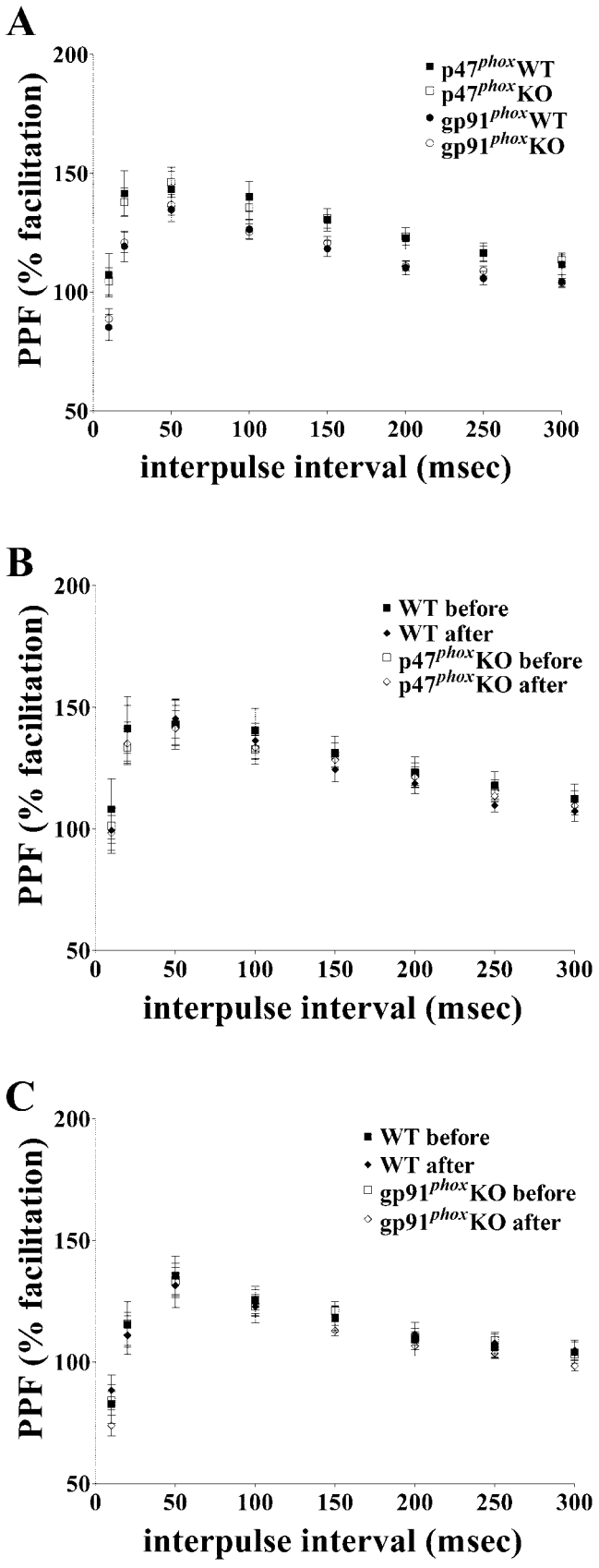

NADPH oxidase does not alter NMDA receptor function in hippocampal area CA1.

PPF is normal in mouse models of CGD. PPF is a short-lasting, presynaptic form of synaptic plasticity that is thought to require residual Ca^{2+} in the presynaptic terminal following the initial pulse (33). It was shown previously that subunits of the NADPH complex colocalize with presynaptic proteins in hippocampal neurons (51), suggesting that NADPH oxidase may play a role in regulating presynaptic function in the hippocampus. Therefore, we tested whether the mouse models of CGD exhibited altered PPF (Fig. 6). Neither the gp91^{phox} nor the p47^{phox} KO mice exhibited differences in PPF compared to their respective wild-type littermates over the range of interpulse intervals tested (Fig. 6A). We also examined whether the deficits in LTP could be related to changes in presynaptic function by testing PPF for 20 min following LTP-inducing HFS. We observed no differences in PPF 20 min after HFS in either line of the NADPH oxidase mutant mice (Fig. 6B and C). These results indicate that NADPH oxidase is not required for this type of short-lasting presynaptic plasticity and suggest that the mechanism underlying the LTP deficit is not likely due to changes in presynaptic function following a single 100-Hz tetanus.

PTP is normal in p47^{phox} KO mice but is impaired in gp91^{phox} KO mice. In our LTP experiments with hippocampal slices from the gp91^{phox} and p47^{phox} KO mice, we noted that there was an immediate impairment in LTP following the high-frequency stimulation (Fig. 2A and C). These results are similar to previous findings in which LTP was blocked immediately by exogenously applied superoxide scavengers (25) and suggest the possibility that PTP, an NMDA receptor-independent form of plasticity, is impaired following HFS. To investigate this possibility, we examined PTP in hippocampal slices from the NADPH oxidase mutant mice. We found no difference in PTP between p47^{phox} KO mice and their wild-type littermates (Fig. 7A). In contrast, we did observe a significant decrease in PTP in gp91^{phox} KO mice compared to their wild-type littermates (Fig. 7A). Interestingly, this effect was mimicked by the application of 10 μM DPI, which inhibits NADPH oxidase via blockade of electron transport in gp91^{phox} (6), to slices from wild-type mice (Fig. 7B). These data are consistent with a role

FIG. 6. Normal paired-pulse facilitation in NADPH oxidase mutant mice. PPF was unaltered in NADPH oxidase mutant mice before (A to C) and after (B and C) receiving a single 1-second 100-Hz train of HFS. The percentage of facilitation, calculated from the ratio of the second fEPSP slope to the first fEPSP slope, is shown at interpulse intervals ranging from 10 to 300 ms ($n = 25$ slices from seven mice for gp91^{phox} wild-type littermates; $n = 24$ slices for seven mice for gp91^{phox} KO and $n = 18$ slices for six mice for p47^{phox} wild-type littermates; $n = 19$ slices for six mice for p47^{phox} KO) ($P > 0.05$, one-way ANOVA). (B) PPF in p47^{phox} KO mice compared to wild-type littermates before and after receiving a single 1-second 100-Hz train of HFS ($n = 9$ slices for six mice for p47^{phox} wild-type littermates; $n = 9$ slices for six mice for p47^{phox} KO) ($P > 0.05$, one-way ANOVA). (C) PPF in gp91^{phox} KO mice compared to wild-type littermates before and after receiving a single 1-second 100-Hz train of HFS ($n = 8$ slices for six mice for gp91^{phox} wild-type littermates; $n = 8$ slices for six mice for gp91^{phox} KO) ($P > 0.05$, one-way ANOVA).

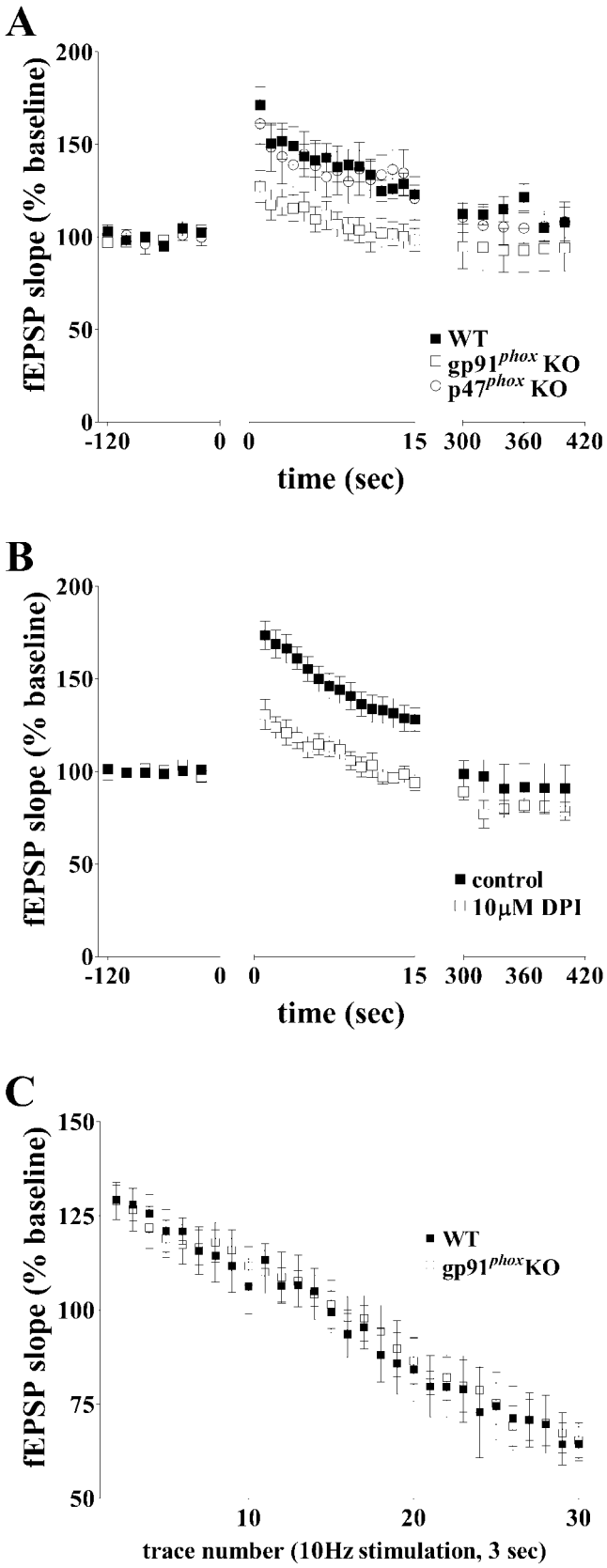

FIG. 7. PTP is normal in p47^{phox} KO mice but decreased in gp91^{phox} KO mice. (A) PTP after a single 1-second 100-Hz train of HFS delivered in the presence of APV (100 μM) was deficient in gp91^{phox} KO mice but was unaltered in p47^{phox} KO mice (n = 13 slices for six wild-type mice; n = 10 slices for three gp91^{phox} KO mice; n = 11 slices for three p47^{phox} KO) ($P < 0.0001$ by one-way ANOVA) (wild-type versus gp91^{phox} KO, $P < 0.001$; wild-type versus p47^{phox} KO, $P > 0.05$; p47^{phox} KO versus gp91^{phox} KO, $P < 0.001$ by Newman-Keuls multiple comparison test). (B) PTP after a single 1-second 100-Hz train of HFS delivered in the presence of APV (100 μM) was deficient in wild-type slices treated with 10 μM DPI. (C) Synaptic fatigue is normal in gp91^{phox} KO mice compared to wild-type littermates. A 3-second 10-Hz train of stimulation was delivered to hippocampal slices prepared from either gp91^{phox} KO or wild-type littermates treated with 100 μM APV. fEPSPs were recorded, and the synaptic fatigue was measured by the steady decrease in fEPSP slope that occurred during the stimulus train. No significant difference was observed between gp91^{phox} KO mice and wild-type littermates ($P > 0.05$, two-way ANOVA).

for gp91^{phox} in PTP that is separable from the role of p47^{phox} in this short-lasting form of synaptic plasticity.

Synaptic fatigue is normal in gp91^{phox} KO mice. In an attempt to gain further insight regarding the PTP deficits we observed in gp91^{phox} KO mice, we assessed synaptic fatigue in these mice using a 10-Hz stimulation that lasted for 3 seconds in the presence of 100 μM APV. During this protocol, fEPSPs recorded in area CA1 were initially potentiated and then rapidly decreased, which is an indication of synaptic fatigue. There were no significant differences in synaptic fatigue between wild-type and gp91^{phox} KO mice (Fig. 7C). These findings indicate that the PTP deficits in the gp91^{phox} KO mice are not due to alterations in synaptic transmission following multiple stimuli. In addition, the fact that PTP is altered in the gp91^{phox} KO mice but not the p47^{phox} KO mice suggests that the functions of these proteins differ with respect to this form of short-lasting plasticity.

Mild hippocampus-dependent memory impairments in mouse models of CGD. It previously was shown that superoxide is required for hippocampus-dependent learning and memory (52, 53). Therefore, we determined whether NADPH oxidase is required for hippocampus-dependent memory by examining the gp91^{phox} and the p47^{phox} KO mice. Specifically, we examined the performance of these mice on two hippocampus-dependent learning and memory tasks: context-dependent conditioned fear and the MWM.

We first tested the p47^{phox} and gp91^{phox} KO mice for memory performance using a conditioned fear paradigm. In this task, the mice learn to fear a new context or an emotionally neutral conditioned stimulus (a tone) because of its association with an aversive unconditioned stimulus (a foot shock). When later exposed to either the same context (hippocampus and amygdala dependent) or the tone (amygdala dependent), the mice freeze, which is the stereotypical fear response used as an index of their memory (11, 39). In a two-trial learning paradigm, the gp91^{phox} KO mice did not show any significant differences from their wild-type littermates in either contextual memory or cued memory (Fig. 8A). We also tested the gp91^{phox} KO mice with a more difficult test for conditioned fear that involved only one training trial; however, these mice still did not exhibit any differences in freezing behavior compared to their wild-type littermates (data not shown). In contrast, the p47^{phox} KO

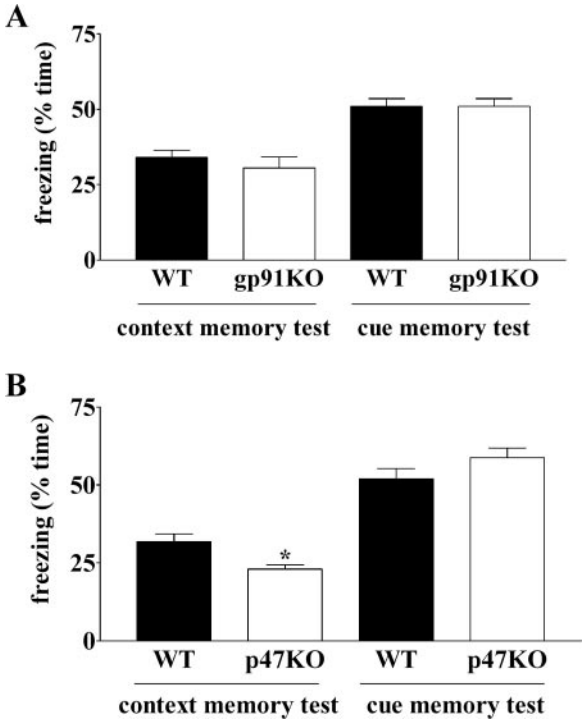

FIG. 8. Conditioned fear memory in NADPH oxidase mutant mice. Mean freezing behavior is shown for contextual and cued fear conditioning tests performed 24 h after training. (A) Wild-type mice versus gp91^{phox} KO mice showed no difference in mean freezing behavior during either the contextual or cued fear response test ($n = 7$ mice per genotype, three cohorts; $P > 0.05$ by Student's two-tailed t test). (B) p47^{phox} KO mice showed a significant decrease in mean freezing behavior during the contextual fear response test ($n = 7$ mice per genotype; * indicates $P < 0.05$ by Student's two-tailed t test) but showed no difference in the cued fear response test ($n = 7$ mice per genotype; $P > 0.05$ by Student's two-tailed t test).

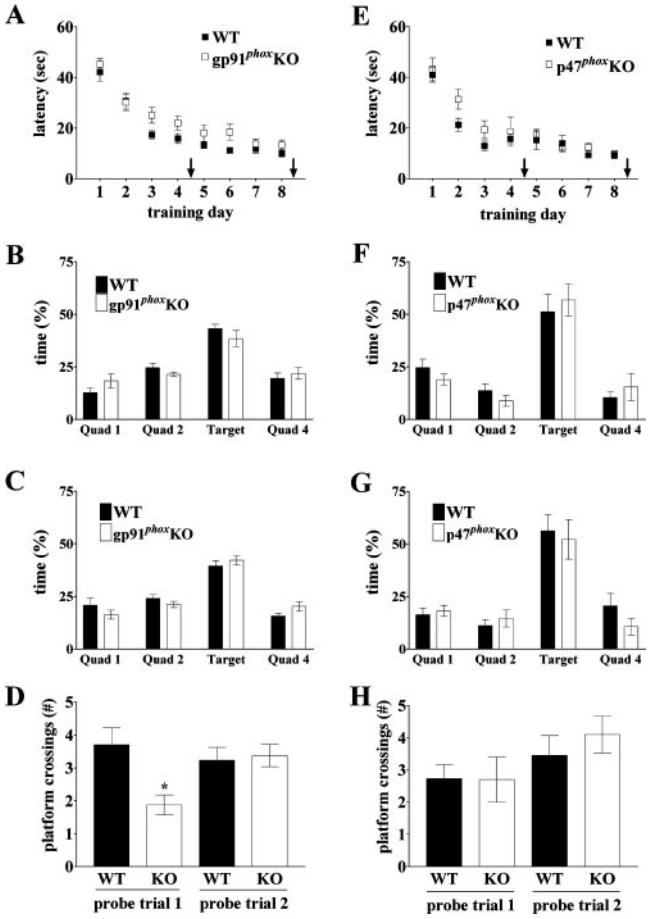

FIG. 9. Morris water maze performance in NADPH oxidase mutant mice. (A to D) MWM performance of gp91^{phox} KO mice compared to wild-type littermates. (A) Escape latencies of gp91^{phox} KO mice versus wild-type littermates were significantly different in the MWM, plotted as a function of training day ($n = 12$ mice per genotype; $P < 0.0001$ by two-way ANOVA). (B and C) Mean proportion of time spent in each of the quadrants during probe test 1 (B) and probe test 2 (C) for gp91^{phox} KO mice versus wild-type littermates ($n = 12$ mice per genotype; $P > 0.05$ by two-way ANOVA). (D) Mean number of platform location crossings during each of the probe trials comparing gp91^{phox} KO mice to wild-type littermates ($n = 12$ mice per genotype) (*, $P < 0.005$ [first probe trial]; P was $\gg 0.05$ for the second probe trial; two-tailed t test). (E to H) MWM performance of p47^{phox} KO mice compared to wild-type littermates. (E) Escape latencies of p47^{phox} KO mice versus wild-type littermates were significantly different in the MWM, plotted as a function of training day ($n = 10$ mice per genotype; $P < 0.0001$ by two-way ANOVA). (F and G) Mean proportion of time spent in each of the quadrants during probe test 1 (F) and probe test 2 (G) for p47^{phox} KO mice versus wild-type littermates ($n = 10$ mice per genotype; $P > 0.05$ by two-way ANOVA). (H) Mean number of platform location crossings during each of the probe trials comparing p47^{phox} KO mice to wild-type littermates ($n = 10$ mice per genotype) ($P > 0.05$ for the first probe trial; $P > 0.05$ for the second probe trial; two-tailed t test).

mice froze significantly less than their wild-type littermates when tested for contextual memory 24 h after training, but they performed similarly to wild-type littermates when tested for cued memory (Fig. 8B). These data are consistent with p47^{phox} being required for the full expression of hippocampus-dependent contextual fear memory, though the effect of losing NADPH oxidase function through the loss of the p47^{phox} subunit appears to be modest. We also tested the gp91^{phox} KO and p47^{phox} KO mice for performance in the MWM in order to assess hippocampus-dependent spatial learning and memory. In this task, the mice must learn and remember the relationship between distal cues and the location of a hidden platform in a pool of water (35). Compared to wild-type littermates, both the gp91^{phox} KO and p47^{phox} KO mice displayed small but significant deficits in their ability to find the platform during early training trials, which improved by the end of the 10-day experiment (Fig. 9A and E). Neither mutant line showed any differences in distance traveled or swim speed throughout the experiment (data not shown). These results are consistent with the interpretation that both lines of NADPH oxidase mutant mice exhibit mild spatial learning impairments.

To assess spatial memory, we tested the mice in two probe trials (on days 5 and 10), in which the platform was removed from the pool and the mice were allowed to search for 60 seconds. The time spent in each quadrant is a measure of the spatial bias of the search pattern employed by the mice. Neither the gp91^{phox} KO nor the p47^{phox} KO mice exhibited any differences compared to their respective wild-type littermates for quadrant preference during either probe trial (Fig. 9B and

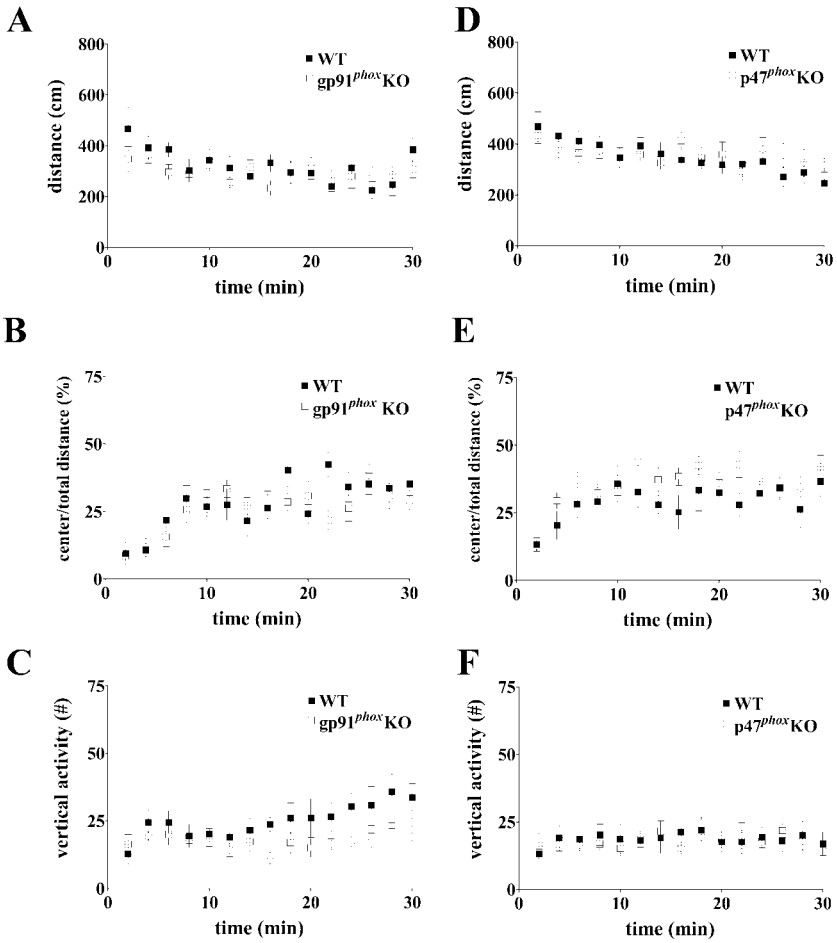

FIG. 10. Open field analysis of NADPH oxidase mutant mice. (A to C) Open field analysis of gp91^{phox} KO mice and wild-type littermates. (A) gp91^{phox} KO mice showed no difference in total distance traveled compared to wild-type littermates ($n = 8$ for gp91^{phox} KO mice and $n = 11$ for wild-type littermates; $P > 0.05$ by two-way ANOVA). (B) gp91^{phox} KO mice showed no difference in their exploration of the center of the open field, expressed as the ratio of center distance to total distance traveled, compared to wild-type littermates ($n = 8$ for gp91^{phox} KO mice and $n = 11$ for wild-type littermates; $P > 0.05$ by two-way ANOVA). (C) gp91^{phox} KO mice reared significantly less than their wild-type littermates, as assessed by the number of vertical beam breaks (vertical activity; $n = 8$ for gp91^{phox} KO mice and $n = 11$ for wild-type littermates; $P < 0.0001$ by two-way ANOVA). (D to F) Open field analysis of p47^{phox} KO mice and wild-type littermates. (D) p47^{phox} KO mice showed no difference in total distance traveled compared to wild-type littermates ($n = 9$ for p47^{phox} KO mice and $n = 8$ for wild-type littermates; $P > 0.05$ by two-way ANOVA). (E) p47^{phox} KO mice showed a slight increase in their exploration of the center of the open field, expressed as the ratio of center distance to total distance traveled, compared to wild-type littermates ($n = 9$ for p47^{phox} KO mice and $n = 8$ for wild-type littermates; $P < 0.0001$ by two-way ANOVA). (F) p47^{phox} KO mice showed no difference in rearing compared to their wild-type littermates as assessed by the number of vertical beam breaks (vertical activity; $n = 9$ for p47^{phox}KO mice and $n = 8$ for wild-type littermates; $P > 0.05$ by two-way ANOVA).

F [probe 1] and C and G [probe 2]). Interestingly, the gp91^{phox} KO mice did show a deficiency during the first probe trial for the number of times they crossed the exact location of the platform, which recovered by the second probe trial (Fig. 9D). The p47^{phox} KO mice did not exhibit any differences in the frequency of platform crossings during either the first or second probe trials (Fig. 9H). Taken together, these data indicate that both the gp91^{phox} and p47^{phox} KO mice display mild spatial learning impairments, and the gp91^{phox} KO mice display mild memory impairments as assessed by the MWM.

OFA in mouse models of CGD. Deficits in the conditioned fear paradigm or the MWM could be caused by differences in exploratory behavior between mutant and wild-type mice. To address this possibility, we assessed the behavior of the gp91^{phox} and p47^{phox} KO mice in the open-field analysis (OFA) paradigm. An OFA tests mice for general exploratory behavior in a novel environment. gp91^{phox} KO mice performed similarly to wild-type mice in both total distance traveled (Fig. 10A) and time spent in the center area relative to the total distance traveled (Fig. 10B), but they reared significantly less than their wild-type littermates (Fig. 10C). These results suggest that gp91^{phox} KO mice for the most part exhibit normal exploratory behavior. Analysis of the p47^{phox} KO mice revealed that these mice performed similarly to their wild-type littermates in total distance traveled (Fig. 10D) and rearing activity (Fig. 10F), but they spent slightly increased time in the center of the arena relative to the total distance traveled (Fig. 10E). Taken together, these results suggest that both mouse models of CGD exhibit largely normal exploratory behavior.

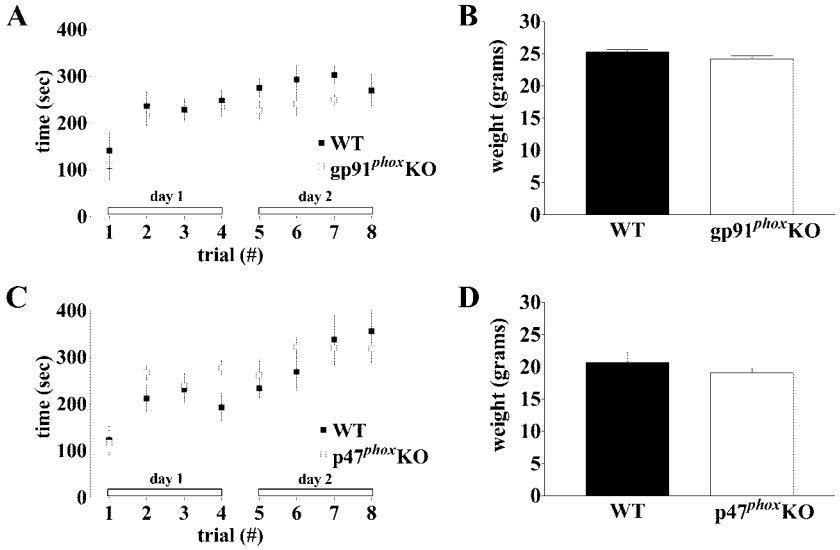

FIG. 11. Rotating rod analysis of NADPH oxidase mutant mice. gp91^{phox} and p47^{phox} KO mice showed largely normal performance on the accelerating rotating rod compared to wild-type littermates. (A) Comparison of gp91^{phox} KO mice and wild-type littermates, measuring time spent balanced on the accelerating rotating rod across eight trials over 2 days. $n = 8$ for wild-type mice, and $n = 11$ for gp91^{phox} KO mice ($P = 0.0268$ by two-way ANOVA). (C) Comparison of p47^{phox} KO mice and wild-type littermates, measuring time spent balanced on the accelerating rotating rod across eight trials over 2 days. $n = 8$ for wild-type mice, and $n = 12$ for p47^{phox} KO mice ($P > 0.05$ by two-way ANOVA). (B and D) Weight comparisons of mutant and wild-type littermates showed no significant difference between knockout mice and wild-type littermates ($P > 0.05$, two-tailed t test).

Motor coordination and motor memory in mouse models of CGD. The accelerating rotating rod tests for motor coordination and motor memory (38). Mice were trained in four trials per day for 2 days to balance on the accelerating rod, and the time they remained on the rod in each trial was recorded. In general, the gp91^{phox} KO mice did not perform as well as their wild-type littermates (Fig. 11A), but the difference was slight and the KO mice performed similar to wild-type mice by the end of training. The p47^{phox} KO mice performed similar to wild-type littermates throughout training (Fig. 11C). The size of the mouse performing this task can significantly affect the performance; however, neither of the mutant mice was significantly different in weight compared to its respective wild-type littermates (Fig. 11B and D). These results suggest that gp91^{phox} KO mice, but not p47^{phox} mice, may have slight impairments in motor coordination and motor memory.

EPM and TST show no differences in the gp91^{phox} KO mice. We also compared the gp91^{phox} KO mice to their wild-type littermates in the elevated plus-maze (EPM) and in the tail suspension test (TST). EPM is a general test for anxiety where exploratory behavior is monitored, and the TST is a simple test that is often used to assess depression. The gp91^{phox} KO did not exhibit any differences compared to wild-type littermate controls in either of these tests (data not shown). These findings indicate that the deletion of gp91^{phox} does not result in generalized anxiety or depression in mice.

DISCUSSION

We have demonstrated that either pharmacological inhibition (Fig. 1) or genetic ablation (Fig. 2) of NADPH oxidase subunits causes deficits in NMDA receptor-dependent E-LTP while leaving basal synaptic transmission intact (Fig. 4). We also found that hippocampal slices prepared from gp91^{phox} KO mice displayed deficient PTP (Fig. 7A), a short-lasting form of synaptic plasticity that is NMDA receptor independent. The E-LTP phenotypes we observed in the gp91^{phox} and p47^{phox} KO mice were correlated with mild impairments in hippocampus-dependent memory (Fig. 8 and 9). These results support the hypothesis that NAPDH oxidase is a source of superoxide that is required for E-LTP and suggest that NADPH oxidase also is required for proper hippocampus-dependent memory function.

Previous studies have shown that superoxide is required for NMDA receptor-dependent LTP (25, 26, 53). Furthermore, NMDA receptor-dependent signaling in the hippocampus, in particular activation of protein kinase C and ERK, requires superoxide (24, 26) and, in the case of ERK activation, a functional NADPH oxidase complex (24). All together, these findings suggest that NAPDH oxidase is an important source of superoxide that is required for activation of signaling cascades that underlie hippocampal LTP.

The source(s) of superoxide required for NMDA receptor-dependent synaptic plasticity in the hippocampus is an open question. Activation of the NMDA receptor results in the production of superoxide (10, 15, 44). In addition to NADPH oxidase, several other sources of superoxide have been implicated previously in LTP, including mitochondria, nitric oxide synthase (NOS), and arachidonic acid. For example, NMDA receptor activation in hippocampal slices has been shown to result in increased production of superoxide via the mitochondrial electron transport chain (4). In addition, in cultured hippocampal neurons mitochondria have been implicated as a source of superoxide that is necessary for activity-dependent

increases in the phosphorylation of cyclic AMP response element binding protein (18), a transcription factor known to be a downstream effector of ERK, both of which are important signaling molecules involved in LTP (50). Also, NOS activity has been shown to be necessary for LTP induction and under certain conditions can generate superoxide that can be blocked by NOS inhibitors (17, 41, 42). Arachidonic acid has also been shown to be a critical messenger molecule during LTP (32), and its metabolism may produce superoxide that is dependent on glutamate receptor stimulation (8, 44) and is required for the induction of LTP (55–57). Finally, NADPH oxidase has been shown to produce large, localized quantities of superoxide (43). The regulation and expression pattern of NADPH oxidase strongly suggest that it could be an important source of superoxide in LTP.

The results presented in this study are the first to directly demonstrate that NADPH oxidase subunits $p47^{phox}$ and $gp91^{phox}$ are necessary for E-LTP (Fig. 1 and 2). Interestingly, previous studies have shown that superoxide was not required for LTP that was induced using multiple trains of HFS; thus, by using a more robust LTP induction protocol, the requirement of superoxide could be overcome. Consistent with this idea, we found that L-LTP was intact in $gp91^{phox}$ KO mice (Fig. 3A) and slightly enhanced in the $p47^{phox}$ KO mice (Fig. 3B) compared to wild-type littermates. Our results provide further evidence that superoxide plays differential roles in E-LTP and L-LTP, with superoxide being required only for E-LTP.

Previous experiments with superoxide-scavenging compounds have shown that there is an immediate decrease in E-LTP following HFS (25, 53). We observed a similar phenomenon in E-LTP experiments in hippocampal slices from $p47^{phox}$ and $gp91^{phox}$ KO mice (Fig. 1 and 2). In addition, we found that the $gp91^{phox}$ KO mice displayed a profound deficit in PTP (Fig. 7A) that was mimicked by the application of DPI, which inhibits the function of $gp91^{phox}$ to wild-type slices (Fig. 7B). These findings indicate that the inhibition of the $gp91^{phox}$ subunit of NADPH oxidase results in not only E-LTP deficits but also impaired PTP. Interestingly, the deficit in PTP was not observed in slices from the $p47^{phox}$ KO mice (Fig. 7A), which together with the enhancement in the L-LTP phenotype (Fig. 3) suggests the possibility that $gp91^{phox}$ contributes to hippocampal synaptic plasticity independent of $p47^{phox}$.

LTP is a physiological phenomenon that models processes thought to underlie memory formation. Many of the molecules that are required for LTP are also required for memory formation, including superoxide. Superoxide has been strongly implicated in hippocampus-dependent memory formation (13, 28, 47, 52, 53). Specifically, mice that overexpress extracellular superoxide dismutase (EC-SOD) show impaired context-dependent fear memory (52, 53) as well as impairments measured in the eight-arm radial maze (28), two assays for hippocampus-dependent memory. Also, mice that overexpress SOD-1 exhibit impaired performance in the MWM (13). Consistent with NADPH oxidase being a required source of superoxide during memory formation, $p47^{phox}$ KO mice showed deficits in contextual fear memory (Fig. 8B); however, $gp91^{phox}$ KO mice showed no deficits in this type of memory (Fig. 8A). On the other hand, $gp91^{phox}$ KO mice showed a mild deficit in spatial memory in the MWM that was overcome with more training (Fig. 9D), whereas both the $gp91^{phox}$ and the $p47^{phox}$ KO mice only exhibited deficits in the latency times during training (Fig. 9A and E). Taken together, these results suggest that $gp91^{phox}$ and $p47^{phox}$ may function independently of one another in certain types of hippocampus-dependent memory.

Compared to previous studies with EC-SOD-overexpressing mice (53), the memory deficits in the NADPH oxidase mutant mice observed are relatively mild. Interestingly, the effects of EC-SOD overexpression on learning seem to have a motivational component (29). At low motivational levels the EC-SOD-overexpressing mice perform the radial arm task poorly, whereas when motivated, they perform the task equal to wild-type mice (29). Because motivation was not examined in the experiments performed here with the NADPH oxidase mutant mice, we cannot rule out the possibility that alterations in motivation are responsible for the memory impairments we have observed.

Both contextual fear and spatial memory require the hippocampus; however, the hippocampus is not sufficient for these behaviors (39). Other brain structures are involved in contextual and spatial memory, and these structures may require $p47^{phox}$ and $gp91^{phox}$ and/or their respective homologues. We obtained evidence that NADPH oxidase is required for behaviors that are hippocampus independent. For example, proper performance on the rotating rod has been shown to require the cerebellar cortex and deep cerebellar nuclei for motor learning and coordination (5). We observed slight differences between the $gp91^{phox}$ KO mice and their littermates in their performance on the rotating rod (Fig. 11A) that may reflect altered function in either the cerebellar cortex or the deep cerebellar nuclei in the mutants. These results suggest that NADPH oxidase may play an important role in synaptic plasticity and function in extrahippocampal areas.

Interestingly, there seems to be a delicate balance of reactive oxygen species (ROS) levels that are required for signaling, whereas too little or too much ROS can result in impairments in LTP and memory (23, 27). Consistent with this hypothesis, there seems to be an age-related shift in the role of ROS signaling in hippocampal LTP and memory formation (19, 23, 27, 30). For instance, in young mice that overexpress SOD-1, LTP is impaired, but this impairment can be rescued with the application of hydrogen peroxide (23). Interestingly, as these mice age, they show an enhancement of LTP that is inhibited by application of H_2O_2 (23), whereas application of H_2O_2 to aged wild-type slices rescues the age-related decline in LTP compared to younger mice (23). EC-SOD transgenic mice also show a similar deficit in LTP at young ages that switches to an enhancement of LTP at older ages (19). Furthermore, chronic treatment of mice with SOD mimetics or catalase mimetics reverses hippocampus-dependent learning deficits in aged mice (30). Thus, the role for ROS in hippocampal plasticity and memory during aging is complex. It will be important for future studies to elucidate the mechanisms underlying the changes in ROS involvement, including the potential changes that are associated with the source and regulation of ROS production during the aging process.

In this study, we have shown for the first time that mouse models of CGD display deficits in synaptic plasticity and mild impairments in cognitive function. CGD has an incidence of between 1:200,000 and 1:250,000 people (58), and identifying the cause of any potential cognitive abnormalities arising in

these patients is important for understanding the molecular mechanisms underlying cognition. Preliminary findings suggest that there may be mild cognitive deficits in patients with CGD (37), consistent with the phenotypes we have observed in the CGD mouse models. Interestingly, there are a number of immunodeficiencies in which patients display cognitive and behavioral abnormalities (37). Many of the molecules implicated as the cause in these immunological diseases are expressed in the nervous system and thus may play a direct role in cognitive function that previously has not been addressed. Identifying the role these molecules play in synaptic plasticity and memory formation will be crucial to our understanding of the molecular mechanisms of cognition.

ACKNOWLEDGMENTS

We thank Richard Paylor and Adrianne Bouwknecht for development of the behavioral core facility at Baylor College of Medicine.

This work was supported by the National Institutes of Health intramural program of the National Institute of Allergy and Infectious Diseases (S.M.H.) and National Institutes of Health grants NS034007 (E.K.), NS047384 (E.K.), and NS047852 (K.T.K.).

REFERENCES

1. **Abramov, A. Y., J. Jacobson, F. Wientjes, J. Hothersall, L. Canevari, and M. R. Duchen.** 2005. Expression and modulation of an NADPH oxidase in mammalian astrocytes. J. Neurosci. **25:**9176–9184.
2. **Babior, B. M., J. D. Lambeth, and W. Nauseef.** 2002. The neutrophil NADPH oxidase. Arch. Biochem. Biophys. **397:**342–344.
3. **Banko, J. L., F. Poulin, L. Hou, C. T. DeMaria, N. Sonenberg, and E. Klann.** 2005. The translation repressor 4E-BP2 is critical for eIF4F complex formation, synaptic plasticity, and memory in the hippocampus. J. Neurosci. **25:**9581–9590.
4. **Bindokas, V. P., J. Jordan, C. C. Lee, and R. J. Miller.** 1996. Superoxide production in rat hippocampal neurons: selective imaging with hydroethidine. J. Neurosci. **16:**1324–1336.
5. **Caston, J., F. Vasseur, T. Stelz, C. Chianale, N. Delhaye-Bouchaud, and J. Mariani.** 1995. Differential roles of cerebellar cortex and deep cerebellar nuclei in the learning of the equilibrium behavior: studies in intact and cerebellectomized lurcher mutant mice. Brain Res. Dev. Brain Res. **86:**311–316.
6. **Clark, S. R., M. J. Coffey, R. M. Maclean, P. W. Collins, M. J. Lewis, A. R. Cross, and V. B. O'Donnell.** 2002. Characterization of nitric oxide consumption pathways by normal, chronic granulomatous disease and myeloperoxidase-deficient human neutrophils. J. Immunol. **169:**5889–5896.
7. **Cross, A. R., and A. W. Segal.** 2004. The NADPH oxidase of professional phagocytes—prototype of the NOX electron transport chain systems. Biochim. Biophys. Acta **1657:**1–22.
8. **Culcasi, M., M. Lafon-Cazal, S. Pietri, and J. Bockaert.** 1994. Glutamate receptors induce a burst of superoxide via activation of nitric oxide synthase in arginine-depleted neurons. J. Biol. Chem. **269:**12589–12593.
9. **Dringen, R.** 2005. Oxidative and antioxidative potential of brain microglial cells. Antioxid. Redox Signal. **7:**1223–1233.
10. **Dugan, L. L., S. L. Sensi, L. M. Canzoniero, S. D. Handran, S. M. Rothman, T. S. Lin, M. P. Goldberg, and D. W. Choi.** 1995. Mitochondrial production of reactive oxygen species in cortical neurons following exposure to N-methyl-D-aspartate. J. Neurosci. **15:**6377–6388.
11. **Fanselow, M. S.** 1984. Shock-induced analgesia on the formalin test: effects of shock severity, naloxone, hypophysectomy, and associative variables. Behav. Neurosci. **98:**79–95.
12. **Ausubel, F. M., R. Brent, R. E. Kingston, D. D. Moore, J. G. Seidman, and K. Struhl (ed.).** 2002. Current protocols in molecular biology. John Wiley & Sons, Inc., New York, N.Y.
13. **Gahtan, E., J. M. Auerbach, Y. Groner, and M. Segal.** 1998. Reversible impairment of long-term potentiation in transgenic Cu/Zn-SOD mice. Eur. J. Neurosci. **10:**538–544.
14. **Groemping, Y., and K. Rittinger.** 2005. Activation and assembly of the NADPH oxidase: a structural perspective. Biochem. J. **386:**401–416.
15. **Gunasekar, P. G., A. G. Kanthasamy, J. L. Borowitz, and G. E. Isom.** 1995. NMDA receptor activation produces concurrent generation of nitric oxide and reactive oxygen species: implication for cell death. J. Neurochem. **65:**2016–2021.
16. **Hancock, J. T., and O. T. Jones.** 1987. The inhibition by diphenyleneiodonium and its analogues of superoxide generation by macrophages. Biochem. J. **242:**103–107.
17. **Heinzel, B., M. John, P. Klatt, E. Bohme, and B. Mayer.** 1992. Ca^{2+}/calmodulin-dependent formation of hydrogen peroxide by brain nitric oxide synthase. Biochem. J. **281:**627–630.
18. **Hongpaisan, J., C. A. Winters, and S. B. Andrews.** 2003. Calcium-dependent mitochondrial superoxide modulates nuclear CREB phosphorylation in hippocampal neurons. Mol. Cell Neurosci. **24:**1103–1115.
19. **Hu, D., F. Serrano, T. D. Oury, and E. Klann.** 2006. Aging-dependent alterations in synaptic plasticity and memory in mice that overexpress extracellular superoxide dismutase. J. Neurosci. **26:**3933–3941.
20. **Hwang, J., A. Saha, Y. C. Boo, G. P. Sorescu, J. S. McNally, S. M. Holland, S. Dikalov, D. P. Giddens, K. K. Griendling, D. G. Harrison, and H. Jo.** 2003. Oscillatory shear stress stimulates endothelial production of O_2^- from $p47^{phox}$-dependent NAD(P)H oxidases, leading to monocyte adhesion. J. Biol. Chem. **278:**47291–47298.
21. **Jackson, S. H., S. Devadas, J. Kwon, L. A. Pinto, and M. S. Williams.** 2004. T cells express a phagocyte-type NADPH oxidase that is activated after T cell receptor stimulation. Nat. Immunol. **5:**818–827.
22. **Jackson, S. H., J. I. Gallin, and S. M. Holland.** 1995. The $p47^{phox}$ mouse knock-out model of chronic granulomatous disease. J. Exp. Med. **182:**751–758.
23. **Kamsler, A., and M. Segal.** 2004. Hydrogen peroxide as a diffusible signal molecule in synaptic plasticity. Mol. Neurobiol. **29:**167–178.
24. **Kishida, K. T., M. Pao, S. M. Holland, and E. Klann.** 2005. NADPH oxidase is required for NMDA receptor-dependent activation of ERK in hippocampal area CA1. J. Neurochem. **94:**299–306.
25. **Klann, E.** 1998. Cell-permeable scavengers of superoxide prevent long-term potentiation in hippocampal area CA1. J. Neurophysiol. **80:**452–457.
26. **Klann, E., E. D. Roberson, L. T. Knapp, and J. D. Sweatt.** 1998. A role for superoxide in protein kinase C activation and induction of long-term potentiation. J. Biol. Chem. **273:**4516–4522.
27. **Knapp, L. T., and E. Klann.** 2002. Role of reactive oxygen species in hippocampal long-term potentiation: contributory or inhibitory? J. Neurosci. Res. **70:**1–7.
28. **Levin, E. D., T. C. Brady, E. C. Hochrein, T. D. Oury, L. M. Jonsson, S. L. Marklund, and J. D. Crapo.** 1998. Molecular manipulations of extracellular superoxide dismutase: functional importance for learning. Behav. Genet. **28:**381–390.
29. **Levin, E. D., F. H. Brucato, and J. D. Crapo.** 2000. Molecular overexpression of extracellular superoxide dismutase increases the dependency of learning and memory performance on motivational state. Behav. Genet. **30:**95–100.
30. **Liu, R., I. Y. Liu, X. Bi, R. F. Thompson, S. R. Doctrow, B. Malfroy, and M. Baudry.** 2003. Reversal of age-related learning deficits and brain oxidative stress in mice with superoxide dismutase/catalase mimetics. Proc. Natl. Acad. Sci. USA **100:**8526–8531.
31. **Lomax, K. J., T. L. Leto, H. Nunoi, J. I. Gallin, and H. L. Malech.** 1989. Recombinant 47-kilodalton cytosol factor restores NADPH oxidase in chronic granulomatous disease. Science **245:**409–412.
32. **Lynch, M. A., M. L. Errington, and T. V. Bliss.** 1989. Nordihydroguaiaretic acid blocks the synaptic component of long-term potentiation and the associated increases in release of glutamate and arachidonate: an in vivo study in the dentate gyrus of the rat. Neuroscience **30:**693–701.
33. **Mohd Noh, L., R. M. Noah, L. L. Wu, B. A. Nasuruddin, E. Junaidah, C. P. Ooi, and I. Rose.** 1994. Chronic granulomatous disease—a report in two Malay families. Singapore Med. J. **35:**505–508.
34. **Morgenstern, D. E., M. A. Gifford, L. L. Li, C. M. Doerschuk, and M. C. Dinauer.** 1997. Absence of respiratory burst in X-linked chronic granulomatous disease mice leads to abnormalities in both host defense and inflammatory response to Aspergillus fumigatus. J. Exp. Med. **185:**207–218.
35. **Morris, R.** 1984. Developments of a water-maze procedure for studying spatial learning in the rat. J. Neurosci. Methods **11:**47–60.
36. **Nauseef, W. M.** 2004. Assembly of the phagocyte NADPH oxidase. Histochem. Cell Biol. **122:**277–291.
37. **Pao, M., E. A. Wiggs, M. M. Anastacio, J. Hyun, E. S. DeCarlo, J. T. Miller, V. L. Anderson, H. L. Malech, J. I. Gallin, and S. M. Holland.** 2004. Cognitive function in patients with chronic granulomatous disease: a preliminary report. Psychosomatics **45:**230–234.
38. **Paylor, R., M. Nguyen, J. N. Crawley, J. Patrick, A. Beaudet, and A. Orr-Urtreger.** 1998. α7 nicotinic receptor subunits are not necessary for hippocampal-dependent learning or sensorimotor gating: a behavioral characterization of acra7-deficient mice. Learning Memory **5:**302–316.
39. **Phillips, R. G., and J. E. LeDoux.** 1995. Lesions of the fornix but not the entorhinal or perirhinal cortex interfere with contextual fear conditioning. J. Neurosci. **15:**5308–5315.
40. **Pollock, J. D., D. A. Williams, M. A. Gifford, L. L. Li, X. Du, J. Fisherman, S. H. Orkin, C. M. Doerschuk, and M. C. Dinauer.** 1995. Mouse model of X-linked chronic granulomatous disease, an inherited defect in phagocyte superoxide production. Nat. Genet. **9:**202–209.
41. **Pou, S., L. Keaton, W. Surichamorn, and G. M. Rosen.** 1999. Mechanism of superoxide generation by neuronal nitric-oxide synthase. J. Biol. Chem. **274:**9573–9580.
42. **Pou, S., W. S. Pou, D. S. Bredt, S. H. Snyder, and G. M. Rosen.** 1992. Generation of superoxide by purified brain nitric oxide synthase. J. Biol. Chem. **267:**24173–24176.

43. **Quinn, M. T., and K. A. Gauss.** 2004. Structure and regulation of the neutrophil respiratory burst oxidase: comparison with nonphagocyte oxidases. J. Leukoc. Biol. **76:**760–781.
44. **Reynolds, I. J., and T. G. Hastings.** 1995. Glutamate induces the production of reactive oxygen species in cultured forebrain neurons following NMDA receptor activation. J. Neurosci. **15:**3318–3327.
45. **Royer-Pokora, B.** 1987. Novel approaches for cloning human genes: the chronic granulomatous disease (CGD). Dis. Markers **5:**57–58.
46. **Serrano, F., N. S. Kolluri, F. B. Wientjes, J. P. Card, and E. Klann.** 2003. NADPH oxidase immunoreactivity in the mouse brain. Brain. Res. **988:**193–198.
47. **Spalloni, A., R. Geracitano, N. Berretta, C. Sgobio, G. Bernardi, N. B. Mercuri, P. Longone, and M. Ammassari-Teule.** 2006. Molecular and synaptic changes in the hippocampus underlying superior spatial abilities in pre-symptomatic G93A$^{+/+}$ mice overexpressing the human Cu/Zn superoxide dismutase (Gly(93)→ALA) mutation. Exp. Neurol. **197:**505–514.
48. **Stolk, J., P. Davies, J. A. Kramps, J. H. Dijkman, J. J. Humes, W. B. Knight, B. G. Green, R. Mumford, R. J. Bonney, and W. A. Hanlon.** 1992. Potency of antileukoprotease and alpha 1-antitrypsin to inhibit degradation of fibrinogen by adherent polymorphonuclear leukocytes from normal subjects and patients with chronic granulomatous disease. Am. J. Respir. Cell Mol. Biol. **6:**521–526.
49. **Sumimoto, H., N. Ueno, T. Yamasaki, M. Taura, and R. Takeya.** 2004. Molecular mechanism underlying activation of superoxide-producing NADPH oxidases: roles for their regulatory proteins. Jpn. J. Infect. Dis. **57:**S24–S25.
50. **Sweatt, J. D.** 2001. The neuronal MAP kinase cascade: a biochemical signal integration system subserving synaptic plasticity and memory. J. Neurochem. **76:**1–10.
51. **Tejada-Simon, M., F. Serrano, L. E. Villasana, B. I. Kanterewicz, G. Y. Wu, M. T. Quinn, and E. Klann.** 2005. Synaptic localization of a functional NADPH oxidase in the mouse hippocampus. Mol. Cell. Neurosci. **29:**97–106.
52. **Thiels, E., and E. Klann.** 2002. Hippocampal memory and plasticity in superoxide dismutase mutant mice. Physiol. Behav. **77:**601–605.
53. **Thiels, E., N. N. Urban, G. R. Gonzalez-Burgos, B. I. Kanterewicz, G. Barrionuevo, C. T. Chu, T. D. Oury, and E. Klann.** 2000. Impairment of long-term potentiation and associative memory in mice that overexpress extracellular superoxide dismutase. J. Neurosci. **20:**7631–7639.
54. **Vallet, P., Y. Charnay, K. Steger, E. Ogier-Denis, E. Kovari, F. Herrmann, J. P. Michel, and I. Szanto.** 2005. Neuronal expression of the NADPH oxidase NOX4, and its regulation in mouse experimental brain ischemia. Neuroscience **132:**233–238.
55. **Watson, J. B., H. Khorasani, A. Persson, K. P. Huang, F. L. Huang, and T. J. O'Dell.** 2002. Age-related deficits in long-term potentiation are insensitive to hydrogen peroxide: coincidence with enhanced autophosphorylation of Ca^{2+}/calmodulin-dependent protein kinase II. J. Neurosci. Res. **70:**298–308.
56. **Williams, J. H., and T. V. Bliss.** 1989. An in vitro study of the effect of lipoxygenase and cyclo-oxygenase inhibitors of arachidonic acid on the induction and maintenance of long-term potentiation in the hippocampus. Neurosci. Lett. **107:**301–306.
57. **Williams, J. H., M. L. Errington, M. A. Lynch, and T. V. Bliss.** 1989. Arachidonic acid induces a long-term activity-dependent enhancement of synaptic transmission in the hippocampus. Nature **341:**739–742.
58. **Winkelstein, J. A., M. C. Marino, R. B. Johnston, Jr., J. Boyle, J. Curnutte, J. I. Gallin, H. L. Malech, S. M. Holland, H. Ochs, P. Quie, R. H. Buckley, C. B. Foster, S. J. Chanock, and H. Dickler.** 2000. Chronic granulomatous disease. Report on a national registry of 368 patients. Medicine (Baltimore) **79:**155–169.